RSC Advances

Cholestatic liver injury model of bile duct ligation and the protection of Huang-Lian-Jie-Du decoction by NMR metabolomic profiling

Journal:	*RSC Advances*
Manuscript ID:	RA-ART-06-2015-012224.R1
Article Type:	Paper
Date Submitted by the Author:	20-Jul-2015
Complete List of Authors:	Wei, Dandan; China Pharmaceutical University, State Key Laboratory of Natural Medicines, Department of Natural Medicinal Chemistry Liao, Shanting; China Pharmaceutical University, State Key Laboratory of Natural Medicines, Department of Natural Medicinal Chemistry Nanjing Wang, Junsong; Nanjing University of Science and Technology, School of Environmental and Biological Engineering Yang, Ming-Hua; China Pharmaceutical University, Department of Natural Medicinal Chemistry Kong, Ling-Yi; China Pharmaceutical University, Department of Natural Medicinal Chemistry

Cholestatic liver injury model of bile duct ligation and the protection of Huang-Lian-Jie-Du decoction by NMR metabolomic profiling

Dandan Wei[a†], Shanting Liao[a†], Junsong Wang*[b], Minghua Yang[a], Lingyi Kong*[a]

[a]*State Key Laboratory of Natural Medicines, Department of Natural Medicinal Chemistry, China Pharmaceutical University, 24 Tong Jia Xiang, Nanjing 210009, PR China. Fax/Tel: 86-25-8327-1405; E-mail: cpu_lykong@126.com*

[b]*Center for Molecular Metabolism, Nanjing University of Science & Technology, 200 Xiao Ling Wei Street, Nanjing 210094, PR China. Tel: 86-25-8431-5512; E-mail: wang.junsong@gmail.com*

*Corresponding author: Prof. Junsong Wang and Prof. Lingyi Kong

† These authors contributed equally to this work

Abstract

Cholestatic liver injury has been increasingly recognized as a cause for high morbidity and mortality of some diseases in human. This model could be established by bile duct ligation (BDL), which led to the toxic accumulation of bile acids in animals, resulting in cholestatic liver injury. In this study, rats were intragastrically administrated with an extract of Huang-Lian-Jie-Du decoction once a day for seven consecutive weeks to study its therapeutic effect. Serum and urine samples were collected and subjected to ^{1}H NMR-based metabolomic analysis. Perturbations on energy metabolism, amino acid metabolism, gut bacteria metabolism and oxidative stress were observed in BDL rats. The metabolomic pattern showed a distinct biphasic feature of BDL model. Most of these metabolic disturbances occured in acute phase (week 1) were greatly attenuated in the long run. HLJDD ameliorated the disturbed metabolism throughout this model, showing bilateral adjustment of some metabolites varied in opposite direction in the two phases. This study demonstrated that ^{1}H NMR-based metabolomics approach is a powerful and feasible tool to study the pathological changes of a disease model dynamically and holistically and for the understanding of the therapeutic effects of complex Chinese herbal medicine formula.

1. Introduction

Chronic cholestatic liver disease is one of the major risks responsible for the development of liver cirrhosis and end-stage liver disease culminating in liver failure. Cholestatic liver disease occurs when there is a decrease in bile flow,[1, 2] which is a

common pathological condition that can be reproduced in rodents by common bile duct ligation (BDL) during surgical laparotomy.[3] Bile acids (BAs) are the active constituents of bile and essential for absorption and solubilization of dietary lipids in the digestive tract.[4] Of them, hydrophobic bile acids could induce damage of mitochondrial membrane structure and increase of oxidative stress, leading to apoptosis in liver cells.[5, 6] The obstruction of bile flow results in an increased accumulation of potentially harmful hydrophobic bile acids in the liver and blood, and liver dysfunction.[7]

Cholestasis is associated with many liver diseases, and a well-established experimental animal model is BDL in rodents, in which hydrophobic bile acid mediated liver injury. This model develops in a biphasic manner, including acute (phase 1) and chronic (phase 2) cholestasis.[8]

Huang-Lian-Jie-Du decoction（HLJDD）is a herbal formula of Traditional Chinese Medicine, consisting of *Coptidis rhizoma, Radix Scutellariae, Cortex Phellodendri* and *Frucuts Gardeniae*. With marked anti-inflammatory activities and the ability to reduce oxidative stress,[9-11] it has been used to treat hepatitis and liver dysfunction.[12] The conventional clinical chemistry and histopathology methods are not region-specific and the sensitivity is relatively low. However, NMR-based metabolomics revealed a global profile of endogenous metabolites, thus performing an overall assessment of the global metabolic state of the entire organism. In this study, an animal model of cholestasis was constructed by BDL and the treatment effect of HLJDD in the BDL model was investigated by a NMR-based metabolomics approach

complemented with histological inspection and biochemical evaluation.

2 Materials & Methods

2.1 Chemicals and kits

Component herbs of HLJDD (*Rhizoma Coptidis, Radix Scutellariae, Cortex Phellodendri* and *Fructus Gardeniae*) were obtained from Jiangsu Medicine Company (Nanjing, China) and authenticated by Professor Mian Zhang, Department of Medicinal Plants, China Pharmaceutical University, Nanjing. The voucher specimens, deposited at the herbarium of the Department of Natural Medicinal Chemistry, China Pharmaceutical University, were 2012066-RC, 2012067-RS, 2012068-CP and 2012069-FG for *Rhizoma Coptidis, Radix Scutellariae, Cortex Phellodendri* and *Fructus Gardeniae,* respectively. 3-Trimethylsilylpropionic acid (TSP) was obtained from Sigma-Aldrich (St. Louis, MO) and deuterium oxide (D_2O, 99.9%) was purchased from QingDao TengLong WeiBo Technology Co. Ltd (QingDao, China). Ultra-pure distilled water was prepared from a Milli-Q purification system. The serum clinical enzymatic chemistry kits of aspartate aminotransferase (AST), alanine aminotransferase (ALT), alkaline phosphatase (ALP), creatinine (CR), total protein (TP), albumin (ALB) and globulin (GLB) were commercially available from Beckman Coulter Inc (Harbor Boulevard, Fullerton, California, 92834 USA), while the serum radioimmunoassay kits of hyaluronic acid (HA), type IV collagen (CIV), type III precollagen (PCIII) and laminin (LN) were bought from Beijing North biology technique institute (Beijing, China).

2.2 Preparation of HLJDD

Rhizoma Coptidis, Radix Scutellariae, Cortex Phellodendri and *Fructus Gardeniae* were mixed in a ratio of 3:2:2:3, reaching a total weight of 500 g. Then they were extracted with 70% ethanol (1:10, 1:10 and 1:5, w/v) under reflux for three times, 1h each, and the extracted solution was filtered through 5 layer gauzes. The decoction was concentrated to dryness to afford 142.5 g HLJDD (yield: 28.5%) using a rotary vacuum evaporator, then stored in refrigerator at 4 °C. The dried extracts were suspended in 0.5% (w/v) sodium carboxy-methylcellulose (CMC-Na) before intragastric administration and the doses were calculated as raw material weights for the animal experiments.

2.3 Bile duct ligation (BDL) operation

BDL was performed using a standard technique.[13] Briefly, animals were anesthetized by injected intraperitoneally (ip) with chloral hydrate (350 mg/kg) and kept under anesthesia with additional ip injection throughout the experiment. After a midline incision under sterile conditions, a single ligature with silk suture was done with 4-0 nylon sutures, followed by careful suturing of the peritoneum and muscle layers as well as the skin wound. The sham-operated rats underwent the same surgical operation except for ligation of bile duct.

2.4 Animals handling procedure

Forty-two adult male Sprague-Dawley rats (220-240 g), of Specified-Pathogens Free (SPF) grade, were obtained from the Experimental Animal Center of Yangzhou University (Yangzhou, China). Rats were group-housed in polysulfone cages (5 rats to one cage) with bedding material, and were housed in a room with controlled humidity

(50 ± 10%) and temperature (25 ± 3 °C) under a 12/12-h light/dark cycle. The animals were given free access to standard diet and water and were allowed to acclimate for 7 days before treatment. The studies were in accordance with the standard guidelines for the Care and Use of Laboratory Animal from the National Institute of Health (NIH) and were approved by the Animal Ethics Committee of the China Pharmaceutical University.

Rats were randomly divided into three groups (n=14): sham-operated (NC), bile duct ligation (BDL) and BDL with HLJDD treatment (BHD). BHD rats were intragastrically administered with HLJDD at doses of 2.7 g/kg body weight, and NC and BDL rats were administered with the same volume of 0.5% CMC-Na for each administration once a day for seven consecutive weeks.

2.5 Collection of serum and urine

On weeks 1, 3, 5 and 7 after the treatment, blood samples were taken from the ocular vein of rats after 12 h fasting. The serum samples were obtained by centrifugation at 13282 g for 10 min, and stored at −80 °C before next experiments. Centrifugation was performed on Beckman Coulter Microfuge® 22R refrigerated microcentrifuge using F241.5 rotor, with a radius of 8.25 cm and the maximum RCF at 21591 g.

Rats were housed in metabolic cages for a 24 hour interval and the urine samples were collected at weeks 1, 3, 5 and 7. The samples were then centrifuged at 13282 g for 10 min to afford the supernatants and stored at −80 °C before NMR spectroscopic analysis.

2.6 Histopathology and serum biochemical analysis

At the end of week 7, rats were fasted overnight and sacrificed after deep anesthetization with chloral hydrate (350 mg/kg, i.p.). The livers and kidneys were removed at the time of death, flushed with cold phosphate buffer solution to remove residual blood. The liver and kidney tissues obtained were immediately immersed in 10% neutral-buffered formaldehyde and embedded in paraffin to be stained with hematoxylin eosin (HE).

Serum samples harvested at different time-points were used for clinical chemistry evaluation. To assess liver and renal function, the concentrations of AST, ALT, ALP, TP, GLB, ALB and Cr were measured using commercially available kits from Nanjing Jiancheng Biotech Inc. On week 7, HA, PCIII, LN and CIV were detected by radioimmunoassay (RIA).

2.7 ^{1}H NMR spectroscopic measurement of serum and urine

The serum and urine samples were thawed at room temperature and 300 μL of each was added with 300 μL D_2O (0.2 mol L^{-1} Na_2HPO_4 and 0.2 mol L^{-1} NaH_2PO_4, pH 7.4, containing 0.05 % TSP). TSP acted as a chemical shift reference (δ 0.0) and D_2O provided a lock signal. The samples were vortexed and centrifuged at 13282 g for 10 min at 4 °C to remove insoluble material. The supernatants were then pipetted out into 5 mm NMR tubes for NMR recording.

^{1}H NMR spectra of the samples were recorded on a Bruker AV 500 MHz spectrometer at 300 K. For each serum sample, the transverse relaxation-edited Carr–Purcell–Meiboom–Gill (CPMG) spin-echo pulse sequence (RD-90°-(τ-180°-τ) n-ACQ) with a total spin-echo delay (2nt) of 40 ms was used to suppress broad signals from

157 macromolecules, therefore the signals of micromolecules were clearly observed. ^{1}H
158 NMR spectra were measured with 128 scans into 32 K data points over a spectral
159 width of 10000 Hz. Prior to Fourier transformation, an exponential window function
160 with a line broadening of 0.5 Hz was used to the free induction decays (FIDs). For
161 urine, a nuclear overhauser effect spectroscopy (NOESY) pulse sequence (relaxation
162 delay-90°-μs-90°-tm-90°-acquire-FID) was used to attenuate the residual water signal.
163 FIDs were collected into 32 k data points over a spectral width of 10000 Hz with an
164 acquisition time of 2.04 s. The FIDs were weighted by an exponential function with a
165 0.3 Hz line-broadening factor prior to Fourier transformation.

166 **2.8 Spectral pre-processing and data analysis**

167 The spectra for all samples were manually phased and baseline corrected, and
168 referenced to TSP at 0.0 ppm, using Bruker Topspin 3.0 software (Bruker GmbH,
169 Karlsruhe, Germany). The ^{1}H NMR spectra were automatically exported to ASCII
170 files using MestReNova (Version 8.0.1, Mestrelab Research SL), which were then
171 imported into "R" (http://cran.r-project.org/), and aligned with an in-house developed
172 R-script to further reduce phase and baseline distortions. The one-dimensional (1D)
173 spectra were converted to an appropriate format for statistical analysis by
174 automatically segmenting each spectrum into 0.005 ppm integrated spectral regions
175 (buckets) between 0.2 and 10 ppm. The region of the residual water and affected
176 signals (4.2–5.7 ppm) was removed. To account for different dilutions of samples, all
177 binned spectra were probability quotient normalized and then mean-centered before
178 further multivariate analysis.

The mean-centered and Pareto-scaled NMR data were analyzed by principal component analysis (PCA) and orthogonal partial least-squares discriminant analysis (OPLS-DA). PCA is an exploratory unsupervised method to maximize the separation by providing model-free approaches for determining the latent or intrinsic information in the dataset.[14] However, no clustering was observed when variables were not selected. OPLS-DA determines PLS components that are orthogonal to the grouping and was used to concentrate group discrimination into the first component with remaining unrelated variations contained in subsequent components.[15] All OPLS-DA models were validated by a repeated two-fold cross-validation method and permutation test. The parameters of R^2 and Q^2 reflected the goodness of fitness and the predictive ability of the models, respectively. The p value of the permutation test denoted the number of times that the permutated data yielded a better result than the one using the original labels. The fold change values of metabolites among different groups were calculated. The Benjamini & Hochberg method[16] was used to adjust the related p-values for controlling the false discovery rate in multiple comparisons applying scripts written in R language, which is available freely, open-source software package.

3 Results

3.1 Animal monitoring

There was no significant difference in the weight of rats in NC, BDL and BHD group on week 7. The serum and urine collected from BDL rats were visually yellow, and after dissection rats undergoing BDL had yellow obstructive jaundice skin, thicken

liver especially in the ventral lobe and enlarged bile duct.

3.2 Liver and kidney histopathology

H&E staining of representative liver sections were observed and shown at 200 × magnifications. The most obvious character of liver impairment after BDL was the severe proliferation of bile duct around the pre-existing interlobular ducts and surrounded by a connective-tissue sheath. Additional diffuse collagen fiber was also noted in interstitial and the portal zones with formation of pseudo lobe. Inflammatory cell infiltration localized specifically to the periportal zones of the livers of BDL rats, was observed in the vicinity of proliferating bile ducts (Figure 1A), as compared with normal livers in the NC group (Figure 1B). Consecutive administration of HLJDD for 7 weeks resulted in remarkable amelioration in these pathological changes (Figure 1C). Histopathological inspection revealed a slight increase of the volume of glomerular in BDL group (Figure 1D) as compared with the NC group (Figure 1E); BHD group showed almost no difference from the normal group (Figure 1F).

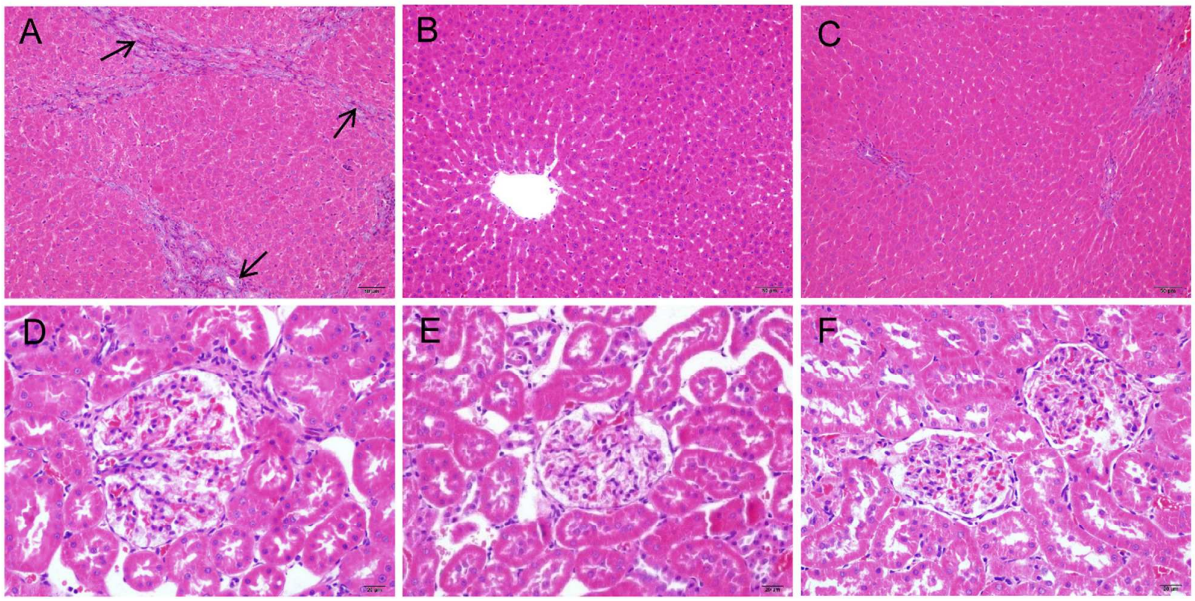

Figure 1. Histopathological study of liver and kidney of NC, BDL and BHD rats at 200 × magnifications. (A) Liver of BDL rats 49 days after operation: exhibiting severe hyperplasia of bile-ducts, inflammatory cell infiltration, and additional diffuse collagen fiber. (B) Livers in sham operation rats: showing no pathological changes. (C) Livers in BHD rats 49 days after intragastric administration: showing no obvious change without any sign of cell degeneration or necrosis. (D) Kidneys of BDL rats after 7 weeks, with slight increase in the volume of glomerular. (E) Kidneys in sham operation group rats, with no pathological changes. (F) Kidneys in BHD group rats after 7 weeks, with no pathological changes.

3.3 Serum biochemical parameters

Serum levels AST, ALT, ALP, CR, TP, ALB and GLB were determined on week 1, 3, 5 and 7, and the results of the clinical chemistry are presented in Fig. 2. Levels of AST, ALT and ALP in BDL group increased significantly on week 1 as compared with the NC group, but the increase attenuated from week 1 onwards, reaching to a minimum on week 7. The elevated AST, ALT and ALP levels indicated that cholestasis and liver cell necrosis were already present one week after BDL[17]. The ALB concentration of BDL rats significant decrease on week 1, 3 and 5, but without significant disturbance on week 7 as compared with NC group. The TP and GLB in BDL group showed some fluctuations throughout the experiments: markedly decreasing on week 1, but markedly increasing on week 3 and 5 and finally kept at normal levels. ALB and GLB, synthesized by liver cells, are indicators of hepatocellular function.[18, 19] The increase of AST, ALT, ALP and decrease of ALB in BDL rats on week 1 indicated a severe cholestatic liver injury in the model.[20] However, variations of these parameters were

attenuated and reversed towards the normal status. On week 7, showing a partial recovery of liver function in BDL rats. The significantly decreased levels of TP, ALB and GLB on week 1 indicated the impaired hepatocellular function in synthesis, and also featuring an acute liver injury. In contrast, on week 3 and 5, both the decrease of ALB and increase of GLB were observed, characterizing chronic liver damage. Similarly, both of them reversed to normal on week 7, indicating the alleviation of liver injury in the long run. The levels of those index indicated liver dysfunction, but HLJDD could restore most of the fluctuations of AST, ALT, ALP, TP, ALB and GLB in the serum. CR in BDL group did not show any significant difference at all time periods.

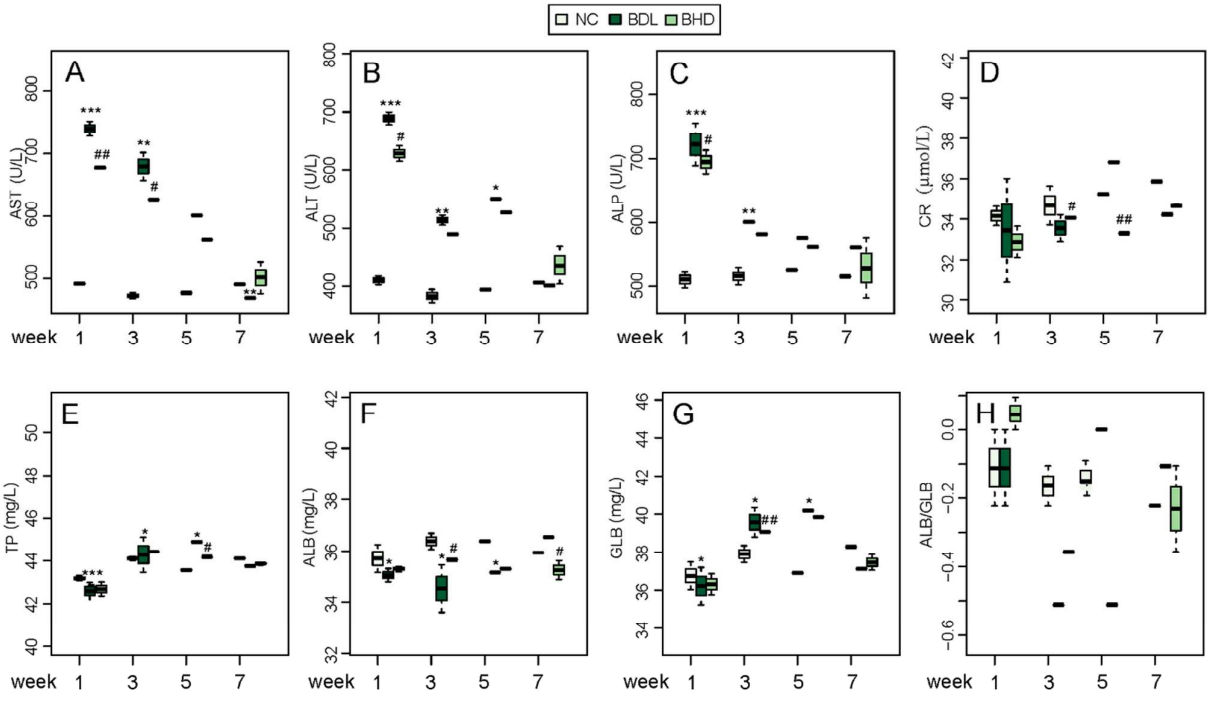

Figure 2. Boxplots of serum levels of creatinine (Cr), total protein (TP), albumin (ALB), alanine aminotransferase (ALT), aspartate aminotransferase (AST), alkaline phosphatase (ALP), globulin (GLB) and the levels of ratio of albumin and globulin (ALB/GLB). The boxes cover 25% quartile

and 75% quartile of the data. The line in the box represents the median value. The extended whiskers show the extent of the rest of the data. (A) AST. (B) ALT. (C) AST_ALT. (D) ALP. (E) CR. (F) TP. (G) ALB. (H) GLB. (I) ALB/GLB. Outliers are shown as open circle. Values were expressed as mean ± SD (n = 10-14). * $p < 0.05$, ** $p < 0.01$ and *** $p < 0.001$ vs. NC rats; $^{\#}$ $p < 0.05$, $^{\#\#}$ $p < 0.01$ and $^{\#\#\#}$ $p < 0.001$ vs. BDL rats.

To asses liver fibrosis, we measured the levels of hyaluronic acid (HA), laminin (LN), type III precollagen (PCIII) and type IV collagen (CIV) in serum (Fig. 3). HA, LN, PCIII and CIV were markers for liver fibrosis.[21] The results revealed that levels of HA and PCIII in BDL rats significantly increased on week 7 ($p < 0.05$), compared with NC rats. The levels of LN and CIV in the serum of BDL group augmented slightly. The results suggested the initial formation of liver fibrosis on week 7. HLJDD could restore increased levels of HA, LN and PCIII in serum.

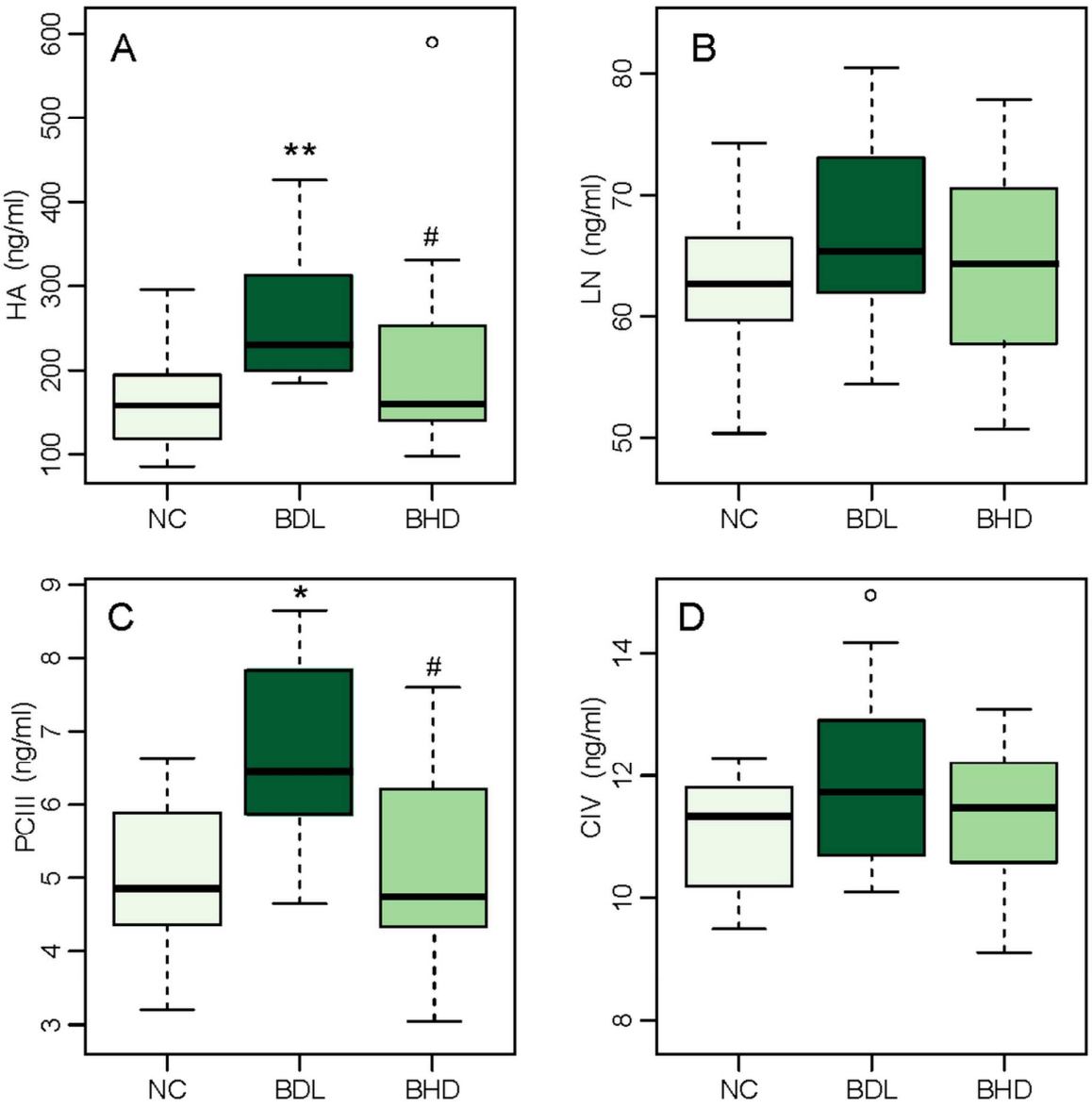

Figure 3. Boxplots of serum levels of hyaluronic acid (HA), type IV collagen (CIV), type III precollagen (PCIII) and laminin (LN) . The boxes and whiskers represent the same as in Figure 2. Boxplots of HA (A), LN (B), PCIII (C), and CIV (D), respectively. Outliers are shown as open circle. Values were expressed as mean ± SD. * $p < 0.05$, ** $p < 0.01$ and *** $p < 0.001$ vs. NC rats; $^{\#}p < 0.05$, $^{\#\#}p < 0.01$ and $^{\#\#\#}p < 0.001$ vs. BDL rats.

3.4 Metabolites identification in serum and urine

Representative 500 MHz ^{1}H NMR spectra of serum and urine samples from NC, BDL and BHD rats were shown in Figures 4 A and B with the assignment of metabolites. Aided by Chenomx NMR suit (Version 8.1, Chenomx, Inc.) and a statistical total correlation spectroscopy (STOSCY) technique,[22] their assignments were made by referencing reported data[16, 23] and querying publicly accessible metabolomic databases, such as HMDB (http://www.hmdb.ca), KEGG (http://www.kegg.jp), METLIN (http://metlin.scripps.edu). The detailed information of the metabolites was listed in Tables S1 and S2.

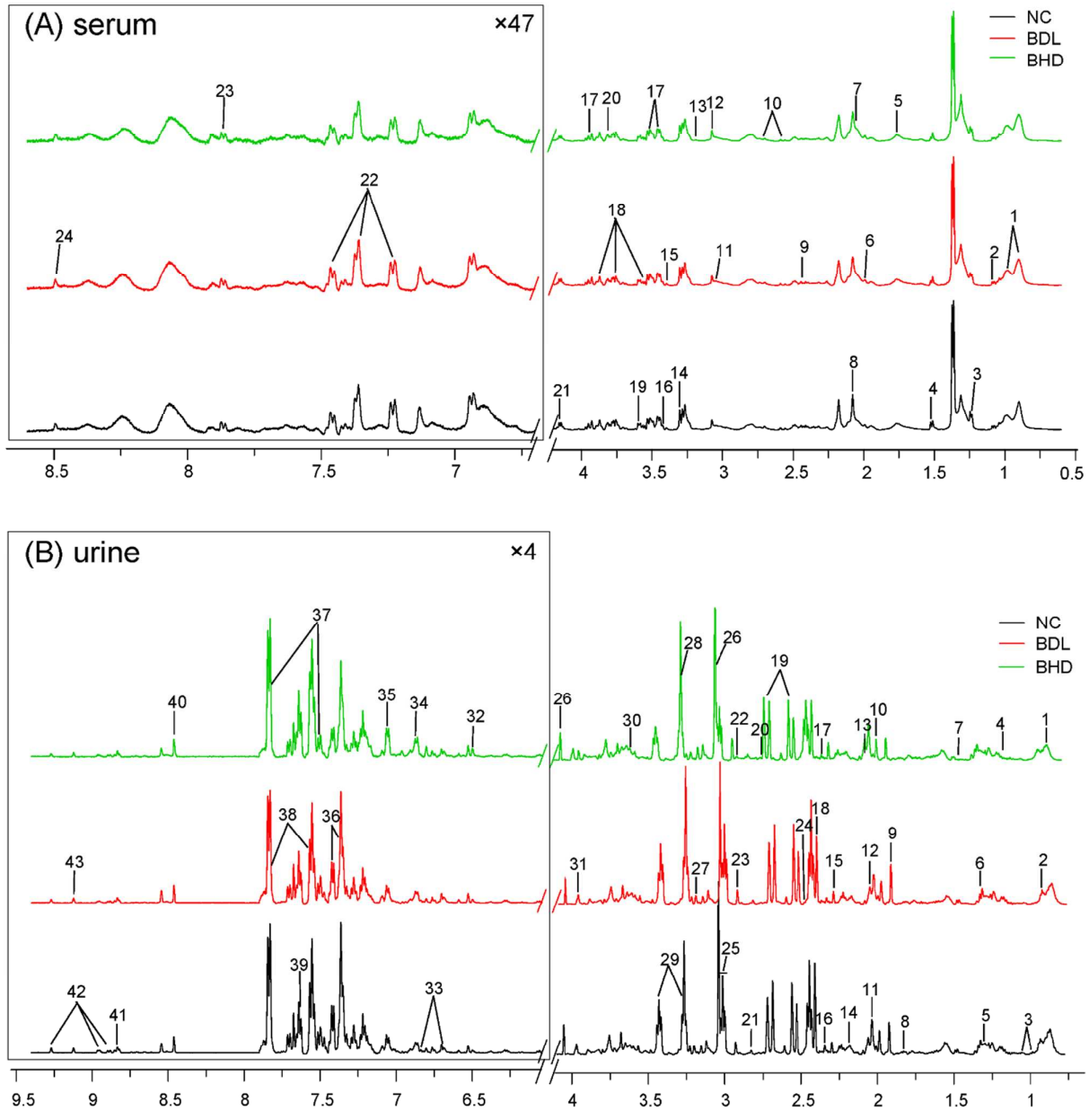

Figure 4. (A) Typical 500 MHz CPMG ^{1}H NMR spectra of the serum samples from NC, BDL and BHD rats on week 1. 1. very low density lipoprotein (VLDL) / low density lipoprotein (LDL); 2. valine; 3. β-Hydroxybutyrate (HB); 4. alanine; 5. lysine; 6. acetate; 7. adipate; 8. N-Acetyl glycoproteins (NAGP); 9. O-Acetyl glycoproteins (OAGP); 10. glutamate; 11.citrate; 12. cysteine; 13. creatine; 14. tyrosine; 15. trimethylamine-N-oxide (TMAO); 16. glycerophosphorylcholine (GPC); 17. taurine; 18. β-glucose; 19. α-glucose; 20. glycine; 21. glutamine; 22. lactate; 23.

phenylalanine; 24. histidine; 25. formate. (B) Typical 500 MHz NOESY ^{1}H NMR spectra of the urine samples from NC rats, BDL rats and BHD rats on week 1: 1. very low density lipoprotein (VLDL) / low density lipoprotein (LDL); 2. isoleucine/leucine; 3. valine; 4. β-Hydroxybutyrate; 5. α-hydroxyisobutyrate; 6. lactate; 7. alanine; 8. ornithine; 9. acetate; 10. proline; 11. N-Acetyl glycoproteins (NAGP); 12. O-Acetyl glycoproteins (OAGP); 13. methionine; 14. adipate; 15. acetoacetate; 16. glutamate; 17. oxalacetate; 18. succinate; 19. citrate; 20. dimethyl amine (DMA); 21. methylguanidine; 22. trimethyl amine (TMA); 23. dimethyl glycine (DMG); 24. pyruvate; 25. 2-oxoglutarate； 26. creatinine; 27. choline; 28. phosphocholine; 29. trimethylamine-N-oxide (TMAO); 30. taurine; 31. glycine; 32. creatine/phosphocreatine; 33. fumarate; 34. 3-hydroxymandelate; 35. 4-aminohippurate; 36. gallate; 37. phenylalanine; 38. tryptophan; 39. benzoate; 40. hippurate; 41. formate; 42. nicotinate; 43. N-methylnicotinamide. 44. NAD^{+}.

3.5. OPLS-DA score trajectory plot at all time points

The metabolic profiles were first subjected to PCA analysis. The three groups showed partial separation from each other in PCA score plots (data not shown) due to the unsupervised nature of PCA. The variations of ^{1}H NMR signals among groups were not only arisen from interested grouping but also from other factors that were group unrelated. To concentrate group discrimination into the first component and filter those variations unrelated to class discrimination, supervised OPLS-DA was further performed.[16] The dynamic metabolic events in the rats were visualized by the OPLS-DA score trajectory plots (Fig.2), where each spot represented the mean position of each group at one time. The direction denoted by arrows represented the

trend of the changing metabolite pattern. The shift of the metabolic patterns in both serum and urine were similar in that BDL group showed the furthest deviation to NC group on week 1, and then moved towards the normal (Fig. 5 A and B). The score trajectory showed a distinct biphasic course of the BDL model. Data on week 1 (acute stage) and week 3 to week 7 (recovery stage) were analyzed independently.

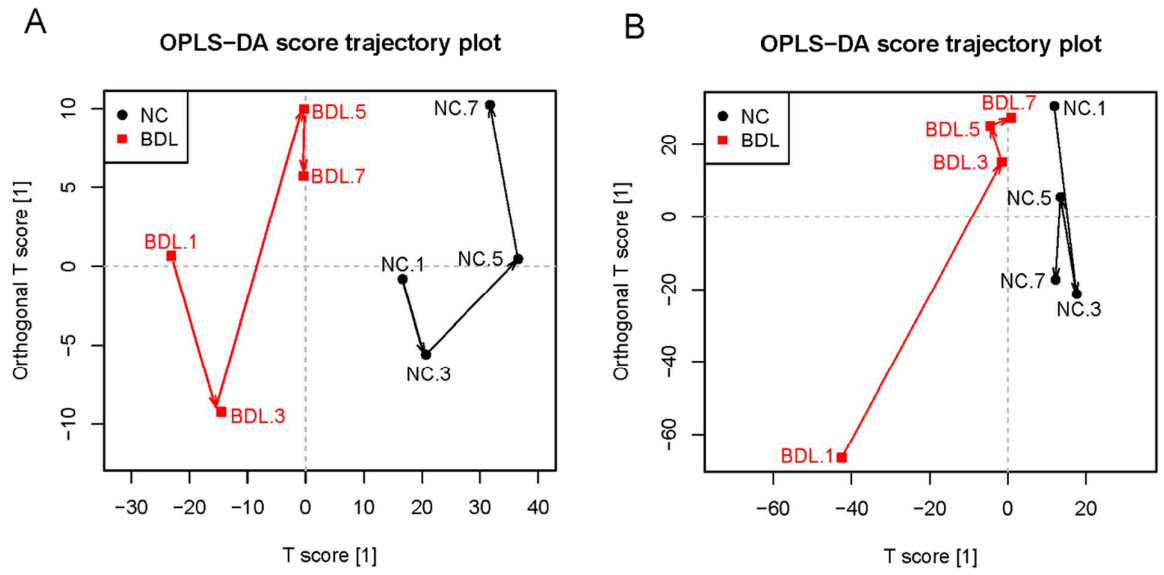

Fig. 5 OPLS-DA score trajectory plots of rats serum (A) and urine (B) of different groups on week 1, 3, 5 and 7 after BDL operation. Symbols of ● (black filled circles), ■ (red filled squares) represented NC and BDL group respectively.

3.6 ^{1}H NMR metabolomics profiles on week 1

3.6.1 Metabolic changes in BDL rats

On week 1, the BDL and NC group showed a complete separation in score plots of serum and urine (Fig. 6 A and C), suggesting a severe metabolic disturbance in BDL groups by a supervised OPLS-DA with a well goodness of fit ($R^2 = 0.93$, $Q^2 = 0.79$; R^2

= 0.98, Q^2 = 0. 93 for the serum and urine, respectively) displayed in Fig. 6 G and H. The corresponding S-plots and loading plots revealed the differential metabolites in serum and urine. In the S-plots, where points in different color and shape represented variables (metabolites), the more further away from the center of a variable, the more contribution of the variable to the class separation of the groups. The loading plots were color-coded with the absolute value of correlation coefficients where red (high coefficients) indicates more marked contribution to the separation than blue (low coefficients) one. The S-plots (Fig.6 B and D) and loading plots (Fig.6 E and F) revealed elevated levels of acetate, creatine, trimethylamine-N-oxide (TMAO), glycerophosphorylcholine (GPC), histidine, phenylalanine in serum; elevated levels of 3-methylglutarate, α-hydroxyisovalerate, isoleucine, leucine, valine, isobutyrate, α-hydroxyisobutyrate, alanine, acetate, trimethylamine (TMA), taurine, N-methylnicotinamide, 3-hydroxymandelate, NAD^+, pyruvate in urine, and lower levels of High density lipoprotein (HDL), alanine, β-glucose, α-glucose, glycine in serum; lower levels of succinate, citrate, dimethylglycine (DMG), creatine/phosphocreatine, creatinine, 2-oxoglutarate, 4-aminohippurate, nicotinate, gallate, hippurate, benzoate, acetylsicylate in urine of BDL rats. These important differential metabolites were further tested for their between-group difference using univariate analysis, and found to be mostly significant as visualized in the heat map (Fig. 8) and fold change plots (Fig. S1).

3.6.2 Effect of HLJDD on the metabolic profiles of BDL rats

To explore the influence of HLJDD on BDL rats, ^{1}H NMR data of serum and urine of

NC, BDL and BHD group were analyzed together. They were clearly separated in the OPLS-DA score plots (Fig. 7 A and C), and BHD groups were in the middle and close to the NC groups, declaring HLJDD can reduce the changes of metabolites caused by the administration of BDL. To find out metabolites that were directly associated with the treatment effect of HLJDD on BDL rats, the metabolic profiles of BDL and BHD groups were analyzed by OPLS-DA (Fig. 7 B and D). The BHD rats were clearly separated from BDL rats with a well goodness of fit (Fig. 7 G and H).

The loading plots (Fig. 7 E and F) revealed great increase of β-glucose, α-glucose, glycine, caprate, glutamine in serum; higher levels of isobutyrate, N-Acetyl glycoproteins (NAGP), O-Acetyl glycoproteins (OAGP), methylguanidine, creatine/phosphocreatine, trimethylamine-N-oxide (TMAO), creatinine, 2-oxoglutarate, threonine, glycine, creatinine, lactate, acetoacetate, β-hydroxybutyrate (3-HB), fumarate, phenylalanine, 4-aminohippurate, 2-oxoglutarate, gallate, NAD^+, benzoate, threonine in urine, and lower levels of LDL, VLDL, adipate, trimethylamine-N-oxide (TMAO) in serum; lower levels of α-hydroxyisovalerate, isoleucine, leucine, valine, alanine, acetate, proline, adipate, dimethyl glycine (DMG), taurine, tryptophan, hippurate, nicotinate, formate, N-methylnicotinamide, 3-hydroxymandelate, NAD^+ in urine of BHD groups. The important differential metabolites selected based on loading plots of OPLS-DA, and found to be mostly significant as visualized in the heat map (Fig. 8) and fold change plots (Fig. S1).

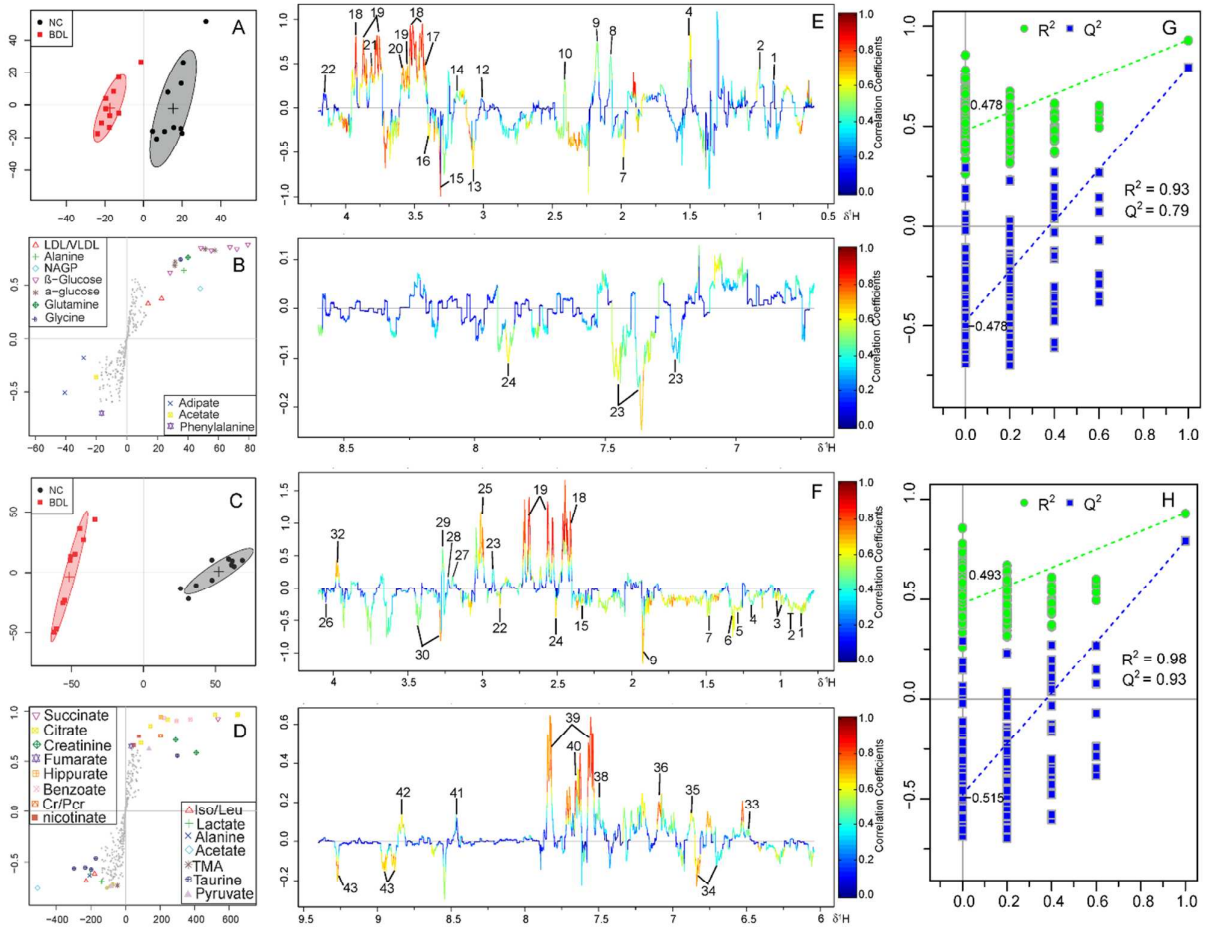

Fig. 6 On week 1, cross-validated OPLS-DA scores plots (A for serum and C for urine), the corresponding S-plots (B for serum, D for urine) and loadings plots (E for serum, F for urine) derived from ^{1}H NMR spectra for NC, BDL and BHD rats. OPLS-DA scatter plot from serum (G) and urine (H) of the statistical validations obtained by 200 times permutation tests, with R^2 and Q^2 values in the vertical axis, the correlation coefficients (between the permuted and true class) in the horizontal axis, and OLS line representing the regression of R^2 and Q^2 on the correlation coefficients.

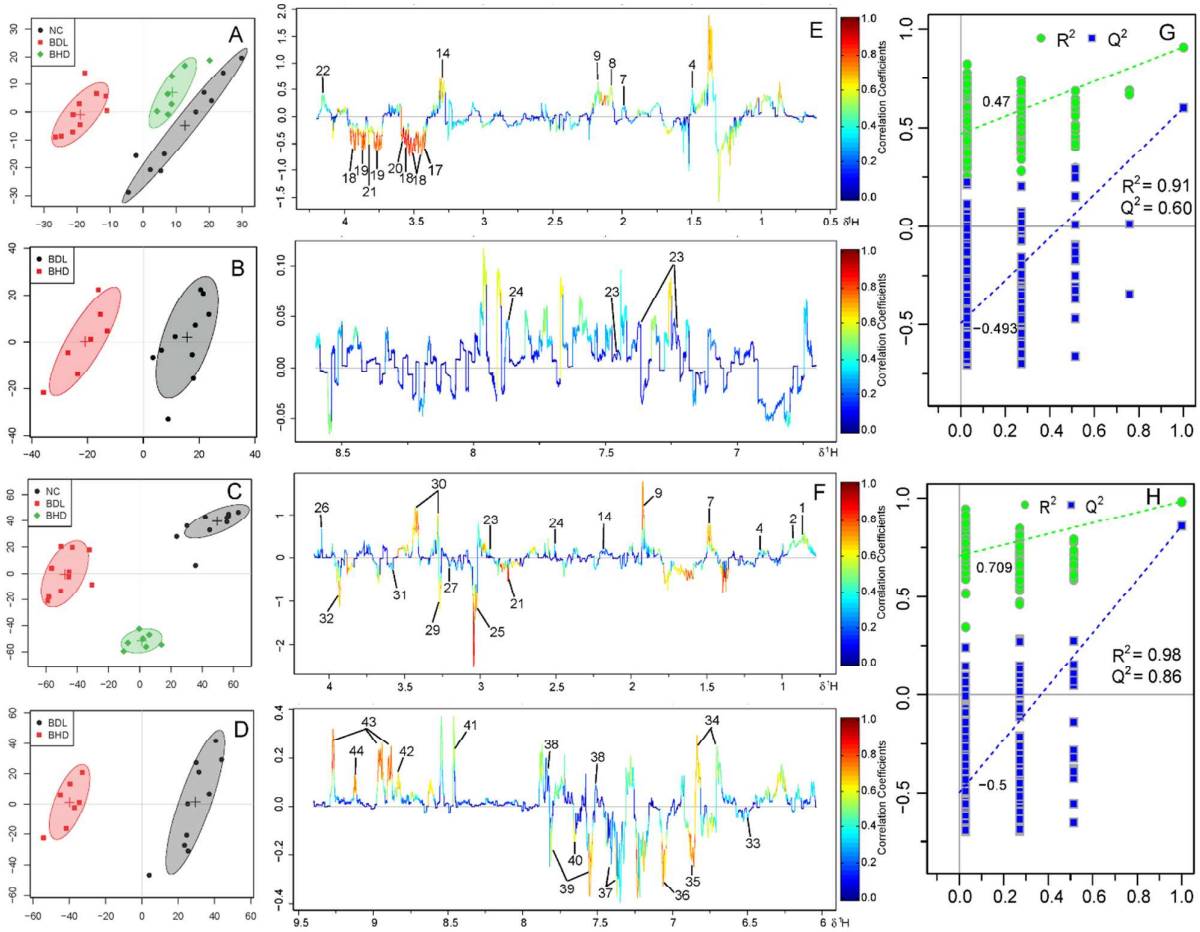

Fig. 7 On week 1, OPLS-DA analysis of ^{1}H NMR data in serum and urine for NC, BDL and BHD group. Scores plots on NC, BDL and BHD rats (A and C), and on BDL and BHD rats (B and D), loadings plots (E and F) for OPLS-DA. OPLS-DA scatter plot from serum (G) and urine (H) of the statistical validations obtained by 200 times permutation tests, with R^2 and Q^2 values in the vertical axis, the correlation coefficients (between the permuted and true class) in the horizontal axis, and OLS line representing the regression of R^2 and Q^2 on the correlation coefficients.

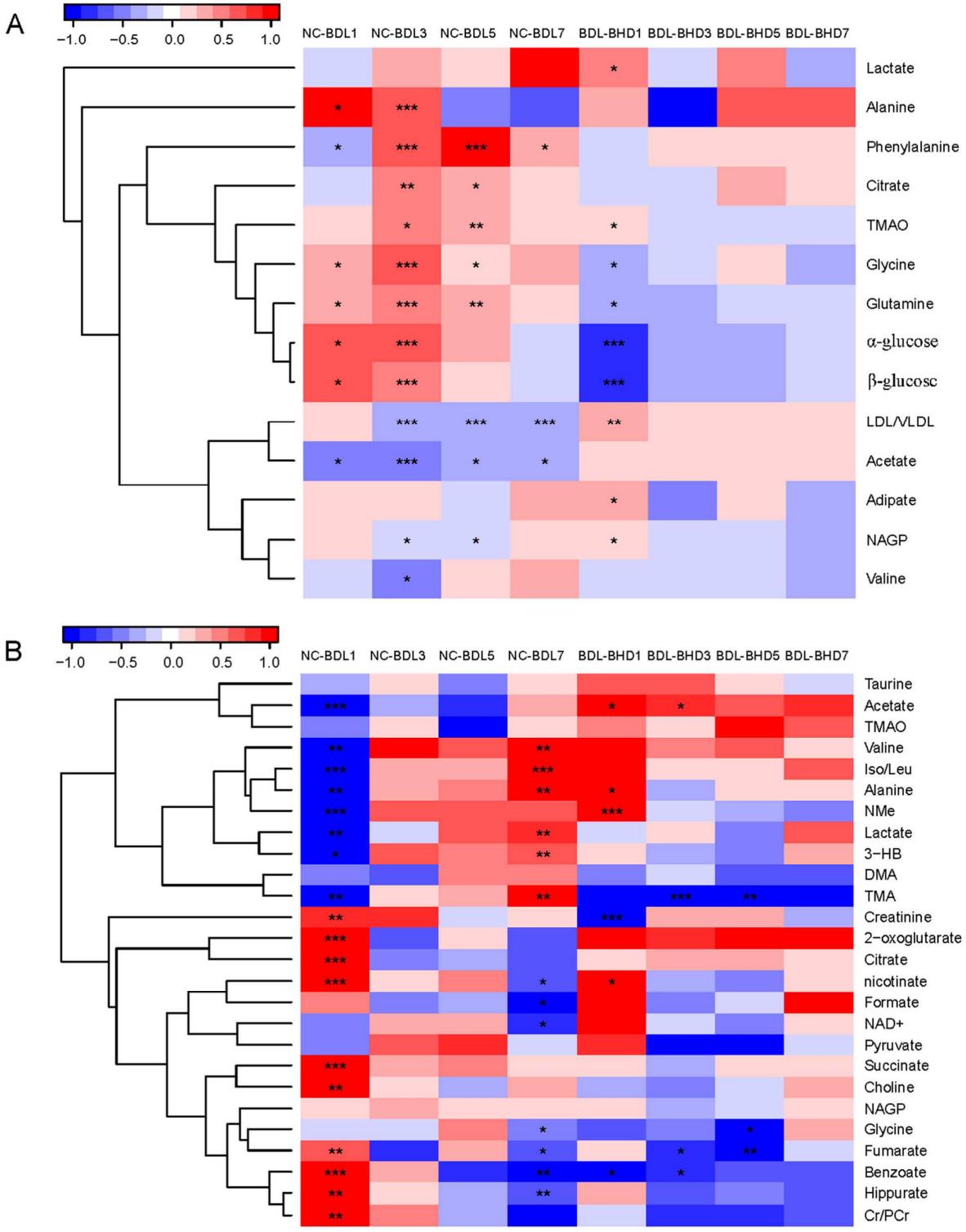

Fig. 8 Heatmap visualization of the z-scored levels of metabolites in serum (A) and urine (B) with stars denoting the differential significance. Row represent metabolites and column represent groups.

385 "BDL" and "BHD" mean "BDL group compare with NC group" and "BHD group compare with
386 BDL group", the number "1", "3", "5" and "7" mean week one, three, five and seven. Color key
387 indicates metabolite quantities value, white: no significant change, deep blue: highest, deep red:
388 lowest, $P< 0.05$ represented statistically significant threshold. * $P< 0.05$, ** $P< 0.01$ and *** $P<$
389 0.001.
390

391 **3.7 ^{1}H NMR metabolomics profiles on week 3, 5, 7**

392 On week 3, 5 and 7, OPLS-DA method was carried out in the BDL, NC, BHD groups.
393 From the score plots of BDL and NC groups (Fig. S2 C and D), revealed a good
394 separation. Compared with NC group, these findings according to the corresponding
395 loading plots (Fig. S3 A, B and C) were observed in BDL group: elevated levels of
396 very low density lipoprotein (VLDL)/low density lipoprotein (LDL), caprate,
397 3-methyladipate/succinyl acetone in serum; elevated levels of citrate, 2-OG in urine,
398 and reduced levels of alanine, lysine, adipate, acetate, glycine in serum; reduced levels
399 of 3-methylglutarate, isoleucine, leucine, valine, α-hydroxyisobutyrate, glutamate in
400 urine of BDL groups. What's more, the OPLS-DA score plots of the serum and urine
401 (Fig. S2 A and B) showed a partial separation of BDL group from NC and BHD group,
402 suggesting damage caused by BDL is gradually restored on week 3, 5 and 7, and NC
403 and BHD group were much overlap in the score plots indicated HLJDD can reduce the
404 changes of metabolites caused by the administration of BDL. Most of the disturbances
405 of metabolites in BDL rats were reversed after treatment of HLJDD (Fig. S2 E,F and
406 Fig. S3 D, E, F).

4 Discussion

In this study, ^{1}H NMR-based metabolomics approach combined with clinical chemistry and histopathology inspection was used to investigate cholestatic liver damage caused by bile duct ligation (BDL) and the treatment effects of HLJDD on BDL rats. Histopathology inspection indicated initial formation of fibrosis in the liver which was testified by the increase of ALT, AST, ALP and decrease of ALB in serum of BDL rats, and the increase of hyaluronic acid (HA), laminin (LN), type III precollagen (PCIII) and type IV collagen (CIV). Slight edema of glomerular was found in the kidney of BDL rats. OPLS-DA analyses of the serum and urinary NMR data of the three groups on week 1, 3, 5 and 7 were performed. The metabolic profiles in BDL rats were severely disturbed, the furthest away from the control on week 1 (acute phase) and then gradually recovered on week 3, 5 and 7 (chronic phase).

One week after BDL operation, rats showed a series of metabolic perturbations, including energy and amino acid metabolism, oxidative stress and intestinal flora disruption.

4.1 Acute phase

4.1.1 Energy metabolism

Significantly decreased levels of urinary citrate, 2-OG, succinate and serum β-glucose, α-glucose together with slightly increased pyruvate level in urine were observed in BDL group as compared with the NC group. Pyruvate is a key intermediate that takes part in both glycolysis and the tricarboxylic acid (TCA) cycle. Generated by

decomposition of glucose, pyruvate can be converted into acetyl-CoA by decarboxylation and enter the TCA cycle under aerobic conditions.[24] The increased level of pyruvate in urine suggested a hampered conversion of pyruvate to acetyl-CoA, which together with notably decreased other intermediates of TCA cycle, citrate, 2-OG and succinate, suggested an inhibition of the TCA cycle.[25, 26] TCA cycle is the most efficient and major source of energy supply. Its inhibition caused energy deficiency, so other means, such as glycolysis, come to rescue. By glycolysis, glucose is converted to lactate by lactate dehydrogenase (LDH) or to alanine by alanine aminotransferase (ALT), resulting in increased lactate and alanine levels.[27] The marked decrease of serum glucose, and increase of lactate and alanine in serum of BDL rats demonstrated an enhanced glycolysis in BDL group.

However, glycolysis is inefficient in energy production. Therefore, ketone bodies metabolism, another means of energy production, have to be enhanced to ameliorate the shortage of energy. Ketone bodies, including acetoacetate and 3-HB, are well-known metabolites of fatty acids in liver mitochondria. Ketones could be transported from serum to muscles, tissues and organs, where ketone bodies could be oxidized to produce energy. The obvious increase of ketone bodies in urine as well as slight decrease of LDL or VLDL in serum of BDL group, suggested an enhanced fatty acid oxidation to produce ketone bodies. As a result, the concentration of acetate, the end product of fatty acid oxidation, was significant increase in the BDL rats. Serum creatine and urinary creatinine were increased in BDL rats. Creatine-phosphate can transfer high-energy phosphate to ADP and produce ATP for energy demand.[28]

Therefore, the significant increase of creatine and its degradation product creatinine suggested a facilitated utilization of creatine-phosphate to replenish energy demand. The increase of creatine and creatinine was also deemed as a sign of hepatic injury,[24] in consistent with pathological result in this study.

BDL rats after HLJDD treatment exhibited markedly enhanced levels of 2-OG, and slightly decreased amount of pyruvate, alanine, 3-HB and acetate, which showcased the ability of HLJDD to ameliorate the disturbed energy supply induced by BDL, possibly by restoration of TCA cycle.

4.1.2 Oxidative stress

Bile acids (BAs) were secreted by hepatocytes, transported into the extracellular matrix in liver and then excreted to duodenum for the absorption and solubilization of dietary lipids. BDL prevented bile flow from liver to duodenum, leading to an accumulation of BAs in liver that generate reactive oxygen species (ROS).[29] The imbalance between the generation of ROS and antioxidant defenses induce oxidative stress.[30] We observed significantly decreased levels of glutamine and glycine and slightly decreased levels of glutamate and cysteine in serum, the precursors of GSH, in BDL rats. GSH as a major natural antioxidant, can react with free radicals directly,[31] thus resisting the damage caused by ROS. The lowered levels of these GSH precursors demonstrated an accelerated GSH synthesis as a consequence of excessive depletion of GSH to counteract ROS.[32]

Urinary choline and phosphocholine were decreased obviously in BDL group compared with the NC group. Phospholipid, consisting of choline and phosphocholine,

is the major component of cell membrane and essential for the maintenance of its integrity.[33] ROS could attack membrane phospholipids, leading to the damage on the construction and function of membranes, and ultimate the rupture of cell and organelles, such as mitochondria.[34] As an evidence, serum levels of NAGP and OAGP were decreased slightly in BDL group since that they were synthesized in membranes of endoplasmic reticulum and golgi apparatus. The lowered levels of choline and phosphocholine indicated an accelerated use of them to renovate the membranes damaged by ROS, thus representing a self-repair mechanism.

HLJDD significantly decreased the elevated urinary level of taurine, and markedly increased the lower serum levels of glutamine, glycine and taurine and urinary choline and phosphocholine in BDL rats, showcasing its protection on BDL induced oxidative injury.

4.1.3 Amino acid metabolism

Taurine and glycine were decreased in serum but increased in urine of BDL rats. BAs could be conjugated to either taurine or glycine in order to reduce the toxicity caused by accumulated BAs. The conjugated BAs were hydrolyzed into free BAs, liberating taurine or glycine under the activation of intestinal bacteria. Normally, most BAs were reabsorbed and, taurine and glycine were excreted into urine.[35] Therefore, the opposite change of taurine and glycine in serum and urine of BDL rats demonstrated accelerated their conjugation with BAs to attenuate the toxicity of accumulated BAs.

Leucine, isoleucine and valine (branched-chain amino acids, BCAAs) were significant increased in urine of BDL rats. ROS induced the decomposition of proteins, resulting

in the damage of cell membrane.[36] BCAAs are important precursors for protein synthesis,[37] and thus essential for the repairment of the damaged cell membranes. The increased excretion of BCAAs in urine of BDL rats showed either an inhibited protein synthesis or an enhanced protein degradation.[38] In addition, these BCAAs can be reabsorbed by glomerular in normal status and their increase may also suggested the dysfunction of glomeruli reabsorption,[39, 40] which also supported by histopathological examination.

Phenylalanine was markedly increased and tyrosine was slightly decreased in serum of BDL rats. phenylalanine is an essential amino acid that has to be obtained from food directly. Tyrosine is a semi-essential amino acid as it can only be synthesized by the hydroxylation of phenylalanine under the catalysis of phenylalanine hydroxylase (PAH). The increased conversion of phenylalanine to tyrosine ratio in BDL group has been observed in patients incurred with hepatitis C virus suffering hepatic damage,[41] and thus may also indicated liver injury induced by BDL operation.

The increased urinary BCAAs, and enhanced conversion of Phe to tyrosine ratio due to BDL operation exhibited a downward trend towards a normal status by the intervention of HLJDD, showing its ability to ameliorate amino acid metabolism and protect rats from BDL induced liver injury.[26]

4.1.4 Intestinal flora metabolism

The levels of hippurate and benzoate were significantly decreased in urine of BDL rats. Benzoate was synthesized from plant phenolics and aromatic amino acids, by intestinal microflora.[42] Benzoate could be absorbed by intestinal tract, eventually

entering into the liver through the portal vein by systemic circulation. BDL prevented the entrance of BAs to intestinal tract, leading to deficiency of intestinal bile salts, and inevitably alteration of gut bacteria,[43] as supported by the obvious decrease of benzoate in urine of BDL rats. As a sequence, the synthesis of hippurate was decreased in BDL group since that hippurate was synthesized by conjugation of glycine with benzoate in the mitochondrial matrix of liver[44, 45] A series of studies have also concluded that the decrease of urinary levels of benzoate and hippurate could be ascribed to the disruption of intestinal flora.[46-48]

The disturbance of gut microbes could also be evidenced by the observed significant increase of trimethylamine (TMA) and partial decrease of trimethylamine (TMAO), since that TMAO is the oxidation product of TMA through the action of gut microbes.[17]

HLJDD significantly increased the levels of urinary TMAO and hippurate, demonstrating a great amelioration of gut microbiota metabolism by HLJDD.

4.2 Chronic cholestasis phase

The severe disturbance in energy metabolism, amino acid metabolism, oxidative stress and gut bacteria in acute phase was greatly attenuated in the long run, characteristic of BDL model. The BDL rats employed a self-repairing process with compensation to address the hampered bile flow by construction of the bypass of bile ducts, which was fully established in BDL rats on week 7.[49]

Interestedly, with no good reasons, levels of urinary citrate, 2-OG and adipate in BDL group were significantly higher than those in NC group, suggesting the complex of the

539 body in response to pathological changes. Surprisingly, these metabolites could also be
540 reversed towards normal levels by HLJDD, in opposite direction to its performance in
541 acute phase, exhibiting a bilateral adjustment of HLJDD.

542 **5 Conclusion**

543 ^{1}H NMR-based metabolomics approach was applied to explore global metabolic
544 features in serum and urine of BDL-induced cholestasis in rats and the treatment
545 effects of HLJDD. The metabolomic pattern showed a distinct biphasic feature of BDL
546 model: acute phase (week 1) and chronic phase (week 3-7). BDL brought severe
547 disturbance in energy and amino acid metabolism, alteration of intestinal flora and
548 oxidative stress in acute phase. The metabolomic results combined with clinical
549 chemistry indicated conspicuous liver dysfunction and the damage of renal glomerular
550 function at acute phase, which were greatly attenuated at chronic phase due to the
551 self-protection mechanism of the body. HLJDD showed bilateral adjustment of some
552 metabolism disturbance. These results demonstrated sensitivity and superiority of
553 metabonomics in disease subtypes and diagnosis, and in the understanding of complex
554 mechanism of a Chinese herbal medicine formula. This integrated metabolomics
555 approach might help to develop a systematic view of BDL-induced injury process and
556 assess its therapy.

557

558 **Acknowledgements**

559 The present study was finally supported by the Key Project of National Natural
560 Science Foundation of China (No. 81430092), the National Natural Science

Foundation of China (No. 81173526) and the Program for Changjiang Scholars and Innovative Research Team in University (PCSIRT-IRT1193).

References

1. M. J. Pollheimer, P. Fickert and B. Stieger, *Molecular aspects of medicine*, 2014, **37**, 35-56.
2. M. Galicia‐Moreno, L. Favari and P. Muriel, *Fundamental & clinical pharmacology*, 2013, **27**, 308-318.
3. S. Ahmadi, Z. Karami, A. Mohammadian, F. Khosrobakhsh and J. Rostamzadeh, *Neuroscience*, 2015, **284**, 78-86.
4. V. Shivanna, Y. Kim and K. O. Chang, *Virology*, 2014, **456-457**, 268-278.
5. D. Sokolovic, J. Nikolic, G. Kocic, T. Jevtovic-Stoimenov, A. Veljkovic, M. Stojanovic, Z. Stanojkovic, D. M. Sokolovic and M. Jelic, *Drug and chemical toxicology*, 2013, **36**, 141-148.
6. T. P. M. d. Sousa, R. E. Castro, S. N. Pinto, A. Coutinho, S. D. Lucas, R. Moreira, C. M. P. Rodrigues, M. Prieto and F. Fernandes, *Biophysical Journal*, 2015, **108**, 242a.
7. B. L. Copple, H. Jaeschke and C. D. Klaassen, Seminars in liver disease, 2010.
8. S. Heinrich, P. Georgiev, A. Weber, A. Vergopoulos, R. Graf and P.-A. Clavien, *Surgery*, 2011, **149**, 445-451.
9. C. B. Li, X. X. Li, Y. G. Chen, H. Q. Gao, P. L. Bu, Y. Zhang and X. P. Ji, *PloS one*, 2013, **8**, e67530.
10. J. Lu, J.-S. Wang and L.-Y. Kong, *Journal of ethnopharmacology*, 2011, **134**, 911-918.
11. X.-b. Wang, Y. Feng, N. Wang, F. Cheung and C.-w. Wong, *Recent patents on food, nutrition & agriculture*, 2012, **4**, 91-106.
12. X. Ye, Y. Feng, Y. Tong, K.-M. Ng, S. Tsao, G. K. Lau, C. Sze, Y. Zhang, J. Tang and J. Shen, *Journal of ethnopharmacology*, 2009, **124**, 130-136.
13. H. Uchinami, E. Seki, D. A. Brenner and J. D'Armiento, *Hepatology*, 2006, **44**, 420-429.
14. S. M. Holand, *http://strata. uga. edu/software/pdf/pcaTutorial. pdf. Last accessed*, 2008, **12**, 2011.
15. J. Boccard and D. N. Rutledge, *Analytica chimica acta*, 2013, **769**, 30-39.
16. J. C. Lindon, R. D. Farrant, P. N. Sanderson, P. M. Doyle, S. L. Gough, M. Spraul, M. Hofmann and J. K. Nicholson, *Magnetic Resonance in Chemistry*, 1995, **33**, 857-863.
17. M. I. Shariff, A. I. Gomaa, I. J. Cox, M. Patel, H. R. Williams, M. M. Crossey, A. V. Thillainayagam, H. C. Thomas, I. Waked and S. A. Khan, *Journal of proteome research*, 2011, **10**, 1828-1836.
18. M. Bernardi, C. S. Ricci and G. Zaccherini, *Journal of clinical and experimental hepatology*, 2014, **4**, 302-311.
19. R. Garcia-Martinez, F. Andreola, G. Mehta, K. Poulton, M. Oria, M. Jover, J. Soeda, J. Macnaughtan, F. De Chiara, A. Habtesion, R. P. Mookerjee, N. Davies and R. Jalan, *Journal of hepatology*, 2015, **62**, 799-806.
20. S. Sathesh Kumar, B. Ravi Kumar and G. Krishna Mohan, *Journal of ethnopharmacology*, 2009, **123**, 347-350.
21. F.-R. Yang, *World Journal of Gastroenterology*, 2010, **16**, 1458.
22. D.-D. Wei, J.-S. Wang, P.-R. Wang, M.-H. Li, M.-H. Yang and L.-Y. Kong, *Journal of pharmaceutical and biomedical analysis*, 2014, **98**, 334-338.
23. A. W. Nicholls, J. C. Lindon, S. Caddick, R. D. Farrant, I. D. Wilson and J. K. Nicholson, *Xenobiotica*, 1997, **27**, 1175-1186.
24. C.-y. Jiang, K.-m. Yang, L. Yang, Z.-x. Miao, Y.-h. Wang and H.-b. Zhu, *PloS one*, 2013, **8**, e66786.
25. S. Satapati, N. E. Sunny, B. Kucejova, X. Fu, T. T. He, A. Mendez-Lucas, J. M. Shelton, J. C. Perales, J. D. Browning and S. C. Burgess, *Journal of Lipid Research*, 2012, **53**, 1080-1092.
26. N. Wang, Y. Feng, H. Y. Tan, F. Cheung, M. Hong, L. Lao and T. Nagamatsu, *Journal of ethnopharmacology*, 2015,

164, 309-318.
27. H. Li, L. Wang, X. Yan, Q. Liu, C. Yu, H. Wei, Y. Li, X. Zhang, F. He and Y. Jiang, *Journal of proteome research*, 2011, **10**, 2797-2806.
28. M. Wyss and R. Kaddurah-Daouk, *Physiological reviews*, 2000, **80**, 1107-1213.
29. P. Ljubuncic, Z. Tanne and A. Bomzon, *Gut*, 2000, **47**, 710-716.
30. X. Cheng, D.-X. Gao, J.-J. Song, F.-Z. Ren and X.-Y. Mao, *Rsc Advances*, 2015, **5**, 4511-4523.
31. I. S. Ovey and M. Naziroglu, *Neuroscience*, 2015, **284**, 225-233.
32. Y.-T. Huang, Y.-C. Hsu, C.-J. Chen, C.-T. Liu and Y.-H. Wei, *Journal of Biomedical Science*, 2003, **10**, 170-178.
33. K. Chingin, J. Liang and H. Chen, *Rsc Advances*, 2014, **4**, 5768-5781.
34. N. Nakamura, *Cells*, 2013, **2**, 732-750.
35. L. Yang, A. Xiong, Y. He, Z. Wang, C. Wang, Z. Wang, W. Li, L. Yang and Z. Hu, *Chemical research in toxicology*, 2008, **21**, 2280-2288.
36. H. Yang, T. W. Li, Y. Zhou, H. Peng, T. Liu, E. Zandi, M. L. Martinez-Chantar, J. M. Mato and S. C. Lu, *Antioxidants & redox signaling*, 2015, **22**, 259-274.
37. A. D. Lake, P. Novak, P. Shipkova, N. Aranibar, D. G. Robertson, M. D. Reily, L. D. Lehman-McKeeman, R. R. Vaillancourt and N. J. Cherrington, *Amino Acids*, 2015, **47**, 603-615.
38. M. Forestier, M. Solioz, F. Isbeki, C. Talos, J. Reichen and S. Krahenbuhl, *Hepatology*, 1997, **26**, 386-391.
39. R. Williams and E. Lock, *Toxicology*, 2005, **207**, 35-48.
40. B. U. Bradford, T. M. O'Connell, J. Han, O. Kosyk, S. Shymonyak, P. K. Ross, J. Winnike, H. Kono and I. Rusyn, *Toxicology and applied pharmacology*, 2008, **232**, 236-243.
41. H. Zoller, A. Schloegl, S. Schroecksnadel, W. Vogel and D. Fuchs, *Journal of Interferon and Cytokine Research*, 2012, **32**, 216-220.
42. H. J. Lees, J. R. Swann, I. D. Wilson, J. K. Nicholson and E. Holmes, *Journal of proteome research*, 2013, **12**, 1527-1546.
43. R. S. Lord and J. A. Bralley, *Alternative Medicine Review*, 2008, **13**, 292-306.
44. C. Lu, Y. Wang, Z. Sheng, G. Liu, Z. Fu, J. Zhao, J. Zhao, X. Yan, B. Zhu and S. Peng, *Toxicology and applied pharmacology*, 2010, **248**, 178-184.
45. J.-Y. Cho, T. Matsubara, D. W. Kang, S.-H. Ahn, K. W. Krausz, J. R. Idle, H. Luecke and F. J. Gonzalez, *Journal of Lipid Research*, 2010, **51**, 1063-1074.
46. J. R. Swann, K. M. Tuohy, P. Lindfors, D. T. Brown, G. R. Gibson, I. D. Wilson, J. Sidaway, J. K. Nicholson and E. Holmes, *Journal of Proteome Research*, 2011, **10**, 3590-3603.
47. Y. L. Wang, H. R. Tang, J. K. Nicholson, P. J. Hylands, J. Sampson and E. Holmes, *Journal of Agricultural and Food Chemistry*, 2005, **53**, 191-196.
48. J. Y. Cho, T. Matsubara, D. W. Kang, S. H. Ahn, K. W. Krausz, J. R. Idle, H. Luecke and F. J. Gonzalez, *Journal of lipid research*, 2010, **51**, 1063-1074.
49. E. Biecker, A. De Gottardi, M. Neef, M. Unternährer, V. Schneider, M. Ledermann, H. Sägesser, S. Shaw and J. Reichen, *Journal of Pharmacology and Experimental Therapeutics*, 2005, **313**, 952-961.